# Structure of $Pt_3Sn(110)$ studied by scanning tunneling microscopy

M. Hoheisel,[1] S. Speller,[1,*] J. Kuntze,[2] A. Atrei,[3] U. Bardi,[4] and W. Heiland[1]
[1]*Fachbereich Physik, Universität Osnabrück, 49069 Osnabrück, Germany*
[2]*Institut für Experimentelle und Angewandte Physik, Universität Kiel, 24098 Kiel, Germany*
[3]*Dipartimento di Sienze e Technologie Chimiche, Università di Siena, I-53100 Siena, Italy*
[4]*Dipartimento di Chimica, Università di Firenze, I-50121 Firenze, Italy*
(Received 22 September 2000; published 24 May 2001)

The (110) surface of the alloy $Pt_3Sn$ is studied by scanning tunneling microscopy, Auger electron spectroscopy, low-energy ion spectroscopy, and low-energy electron diffraction. Preferential sputtering of the surface causes depletion in Sn in the surface region. Annealing at 600 K leads to the formation of a hill-and-valley structure with {102} facets perpendicular to the close packed $[\bar{1}10]$ surface rows. After annealing at 1000 K large terraces are formed with a bulk-terminated structure and well-defined steps. Of the two possible terminations, i.e., pure Pt or PtSn, the Sn rich surface is clearly favored.

DOI: 10.1103/PhysRevB.63.245403 PACS number(s): 68.35.Bs

## INTRODUCTION

The $Pt_3Sn$ alloy belongs to the chemically ordered $L1_2$ group of alloys. The surfaces of this alloy are of interest owing to its catalytic properties.[1–3] In the equilibrium state the surfaces studied are always chemically ordered but depending on the preparation they show a variety of reconstructions, superstructures, etc.

Previously, we reported results from the (111) and (001) surfaces of $Pt_3Sn$.[4,5] On the (111) surface scanning tunneling microscopy (STM) studies revealed a mesoscopic honeycomb network not found previously by low-energy electron diffraction (LEED) and low-energy ion scattering (LEIS),[6–9] quantitative LEED analysis,[9,10] and x-ray photoelectron diffraction.[11] This honeycomb network is due to buried dislocations which in turn are caused by Sn depletion in the surface region as a consequence of the preferential sputtering of Sn. The other structures typical for the (111) surface, i.e., the $p(2\times2)$ and the $(\sqrt{3}\times\sqrt{3})R30°$ structures, are found by all these structural analysis methods. The (001) surface poses more problems due to the observation of ''streaky'' LEED patterns at intermediate preparations which are hard to analyze.[6–9] The STM analysis resolved the problem by finding pyramidal structures with {102} and {104} facets on this Sn depleted surface that cause the streakiness in the LEED patterns.[5]

The (110) surface has been studied in less detail so far. The Sn/Pt LEIS intensities after annealing at 1000 K turned out to be similar for the (001) and (110) surfaces, and twice that for the (111) surface.[12] The LEED patterns reported are streaky, $(1\times1)$, $(2\times1)$, or rhombic depending on the state of preparation.[6,7,12] In the LEED nomenclature $(2\times1)$ means that in the top $[\bar{1}10]$ rows of the (110) surface Pt and Sn atoms are alternating, i.e., the surface is bulk terminated [Figs. 1(a) and 1(b)]. This is in contrast to, e.g., the clean surfaces of Pt(110), Au(110), or $Au_3Pd(110)$ which are $(1\times2)$ reconstructed in the so called missing-row structure.[13,14] $Pt_3Sn$ has a lattice constant of $a_0=4.00$ Å; this is slightly larger than that of pure Pt at 3.92 Å.

In the present paper we report results of a STM, LEED, auger electron spectroscopy (AES), and LEIS study of the clean $Pt_3Sn(110)$ surface.

## EXPERIMENT AND RESULTS

The experiments except for LEIS were performed in an ultrahigh-vacuum (UHV) system in Osnabrück at a base pressure below $5\times10^{-11}$ mbar. The main features of the setup are an Omicron STM I system, a LEED (reflection high-energy electron diffraction) system, an 180° electrostatic analyzer for AES, and stages for sputtering and annealing of the samples. For the sputtering a clean $Ar^+$ ion beam at an energy of 600 eV is used. The annealing temperature is monitored with a thermocouple. The LEIS spectra were acquired in an UHV system in Firenze. A Varian ion gun is used for sample cleaning and the LEIS measurements. The analysis ion beam current is of the order of $1\times10^{-8}$ A. The chamber is equipped with a hemispherical electron/ion energy analyzer (HA100, Vacuum Science Workshop).

The AES spectra acquired after sputtering (Fig. 2) indicate the usual depletion in Sn within the upper layers. After some minutes at few microamperes ion bombardment the

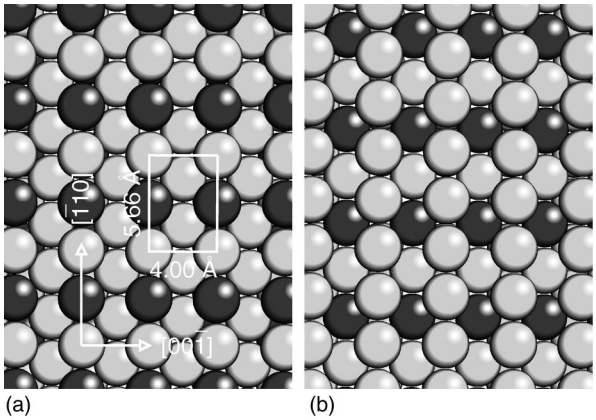


FIG. 1. Sphere models of the two possible bulk terminations of $Pt_3Sn(110)$. Dark gray spheres represent Sn atoms, and light gray spheres represent Pt atoms.

 

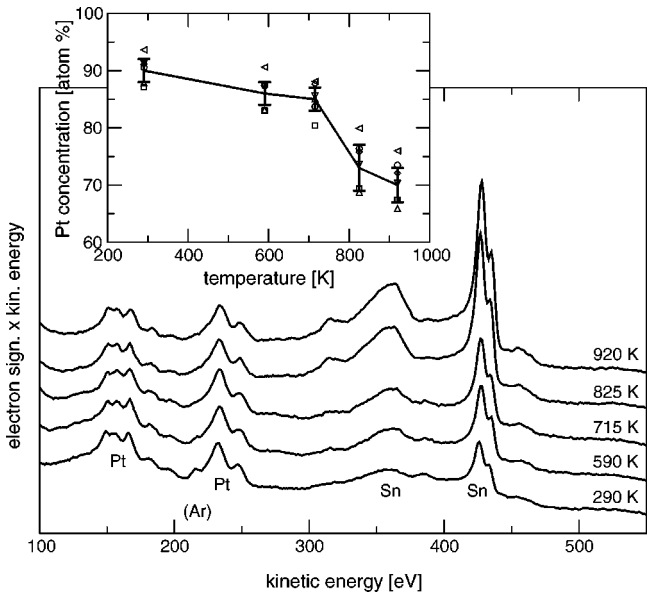


FIG. 2. AES spectra after sputtering (bottom curve) and subsequent annealing (higher curves). Each annealing temperature was kept until no further changes in the signal were observed. The AES spectra were taken at a primary electron energy of 10 keV. The inset shows the variation of the Pt concentration with temperature. The concentration values were calculated on the basis of AES sensitivity factors.

depletion is saturated. Annealing up to 1000 K restores the Sn signal to a steady state level, i.e., further annealing does not change the peak height ratio between Sn and Pt. This evolution of the composition in the surface region according to AES (see inset of Fig. 2) is very similar to that of the $Pt_3Sn(001)$ surface.[5] In contrast to AES, the LEIS spectra yield a totally different development of the Sn concentration in the topmost layers (Fig. 3). The outermost layers are much less depleted in Sn after sputtering than is the surface region. After annealing at 600–900 K there is more than 50% Sn in

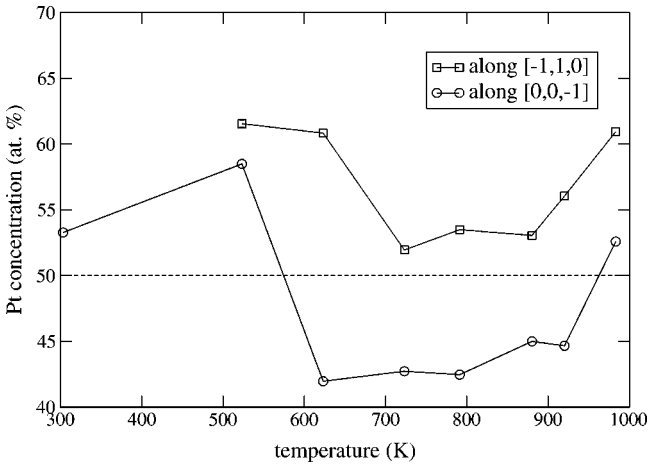


FIG. 3. Pt concentration in the outermost layers determined by LEIS. The measurements were taken after sputtering and subsequent annealing. The He beam (1 keV) impinges on the sample surface with an angle of 45°; the scattering angle is 135°. The ions impinged along the indicated azimuthal directions.

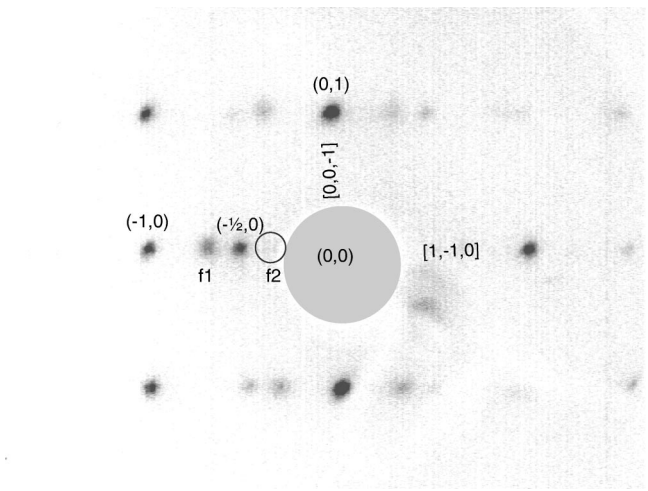


FIG. 4. LEED image of the faceted surface after 600 K anneal at 83 eV electron energy. The diffraction pattern contains the $(1\times1)$, $(2\times1)$, and facet beams (labeled $f1$ and $f2$). With varying energy the intensity of the facet beams shifts between the positions $f1$ and $f2$.

the outermost layers. Further annealing at 1000 K decreases the amount of Sn to about 50%. A similar behavior was found on the $Pt_3Sn(111)$ surface, where after annealing at intermediate temperatures a Sn enriched layer over a Sn depleted surface region is observed.[4,9]

In the interesting temperature range around 600 K a LEED pattern indicating faceting is observed (Fig. 4). The extra beams appear along $[\bar{1}10]$ at 1/3 positions with respect to the $(2\times1)$ pattern. With varying electron energy pairs of extra beams (see, e.g., beams $f1$ and $f2$ in Fig. 4) appear and change their intensity alternately. The corresponding STM topographic image indeed reveals a faceted surface [Figs. 5(a) and 5(b)]. The facets can be identified as {102} faces as shown in the model [Fig. 5(c)]. The model shows a non-bulk-terminated variant of the {102} facet (see the arguments below). The {102} planes are tilted $\pm18.4°$ with respect to the (110) plane and the distance between adjacent $[00\bar{1}]$ rows in the {102} facets is $1.5\times a_0/\sqrt{2}=4.24$ Å. Thus the shortest possible period of up and down sequences out of {102} minifacets is 8.5 Å in accordance with the observations [Fig. 5(b)]. There is no straightforward argument why the {102} planes are favored. Please note that the pyramids on $Pt_3Sn(001)$ also displayed {102} facets.[5]

With higher-temperature annealing (1000 K) the facets gradually disappear and large flat terraces develop [Fig. 6(a)] until they are the dominant structure [Fig. 6(b)]. The steps on the well annealed surface are of double height (2.8 Å) or multiples of double height, i.e., always even number steps [see height scans in Figs. 6(c) and 6(d)]. Double steps have to be expected if the crystal surface is bulk terminated with only one type of surface layer exposed [Fig. 1(a) or 1(b)]. The minifacets of the $[00\bar{1}]$ steps display slopes of 18.4° with respect to the (110) plane [Fig. 6(c)]. Thus, these facets are {102} oriented like the facets in the hill-and-valley-like structure [Fig. 5(a)]. The apparent slope of the facets at the $[\bar{1}10]$ double steps is 22.5° on average [Fig. 6(d)]. This is

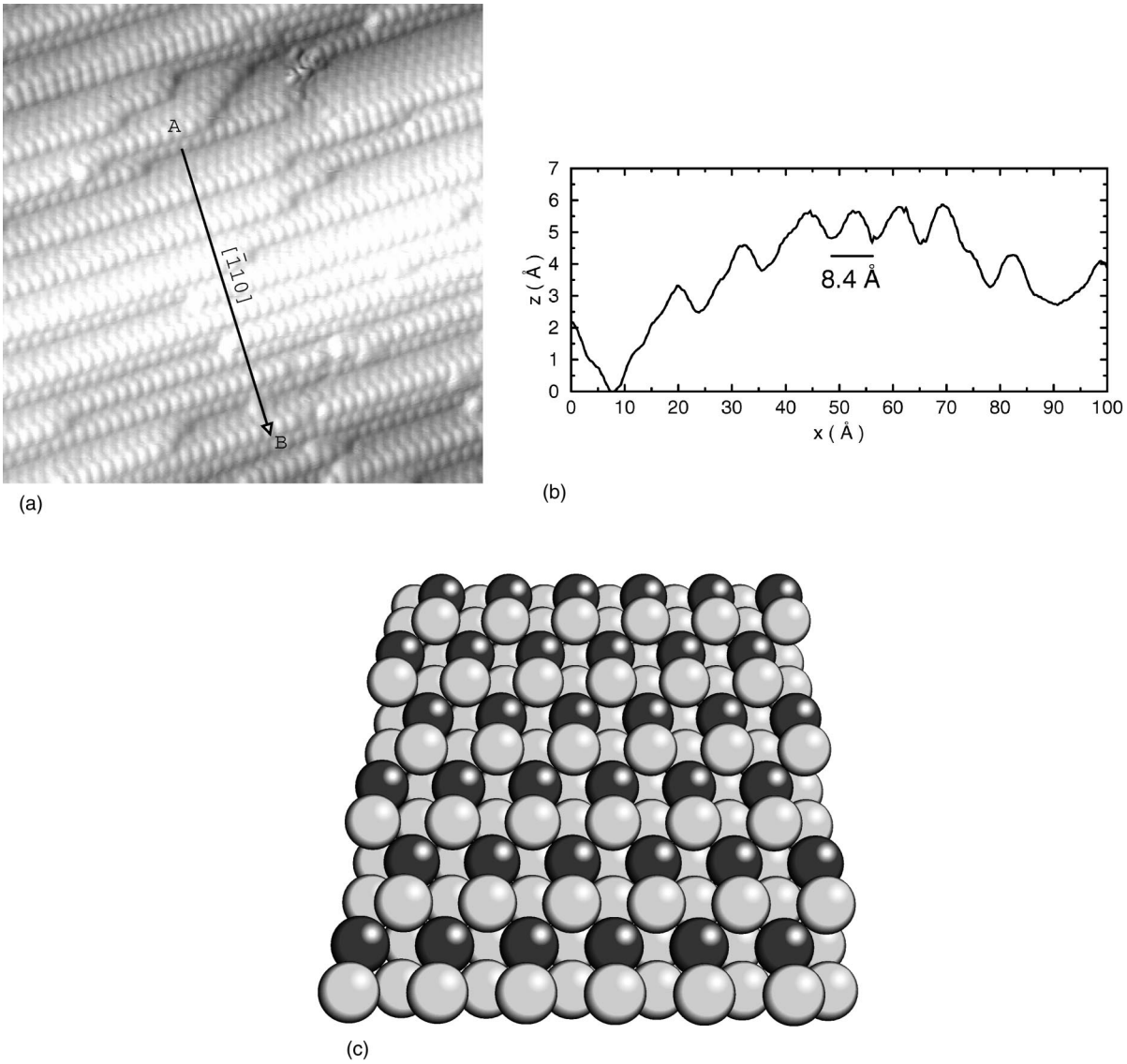


FIG. 5. STM image of the {102} facets after anneal to 715 K, 154 Å, −0.15 V, 2.5 nA (a), height scan between *A* and *B* along $[\bar{1}10]$ (b), and sphere model of a non-bulk-truncated {102} facet, which is in accordance with the data.

smaller than expected for the usual {111} minifacet orientation, i.e., 35° with respect to the (110) plane. Since $[\bar{1}10]$ steps occur only with double height we attribute the smaller angle to Smoluchowski smoothing and resolution limits of the tip.

The higher stability of larger {102} facets can be seen more clearly at places where two or more double steps merge [circles in Figs. 7(a) and 7(b)]. The tendency of double steps to merge to multiple double number steps is obviously stronger for the $[00\bar{1}]$ steps than for the $[\bar{1}10]$ steps as visible in Fig. 7(a) (circles). The atomic corrugation at the facets of two fourfold steps is visible in the STM image shown in Fig. 7(b).

The question of whether the $Pt_3Sn(110)$ surface is in the Sn rich or in the Pt rich state [Figs. 1(a) and 1(b)] can be answered by looking at high-resolution STM images (Fig. 8). Since we know the orientation of the crystal from the LEED patterns we can identify the $[\bar{1}10]$ direction in the STM topograph. Clearly, in the STM images the surface lattice distance is larger along the $[\bar{1}10]$ direction than along the $[00\bar{1}]$ direction. This agrees with the $(2\times1)$ reconstruction indicated by LEED, taking into account the poor visibility of the Sn atoms as was found on the (111) and (001) surfaces.[4,5] This contrast occurs because the surface density of states at the Fermi edge is significantly lower for Sn than for Pt.[5,23] Thus, the surface structure in the equilibrium phase is represented by the model of Fig. 1(a), i.e., bulk terminated in the Sn rich state.

{102} planes of different composition are stacked alternately such that bulk-terminated {102} facets can exhibit either pure Pt or mixed PtSn layers, as with {001} and {110} planes. However, the observed structure at the facets is incompatible with both bulk terminations. A pure Pt termination can be excluded because of the LEIS results. Further, we can exclude the mixed PtSn termination for the following reasons. The observed distance between adjacent atomic

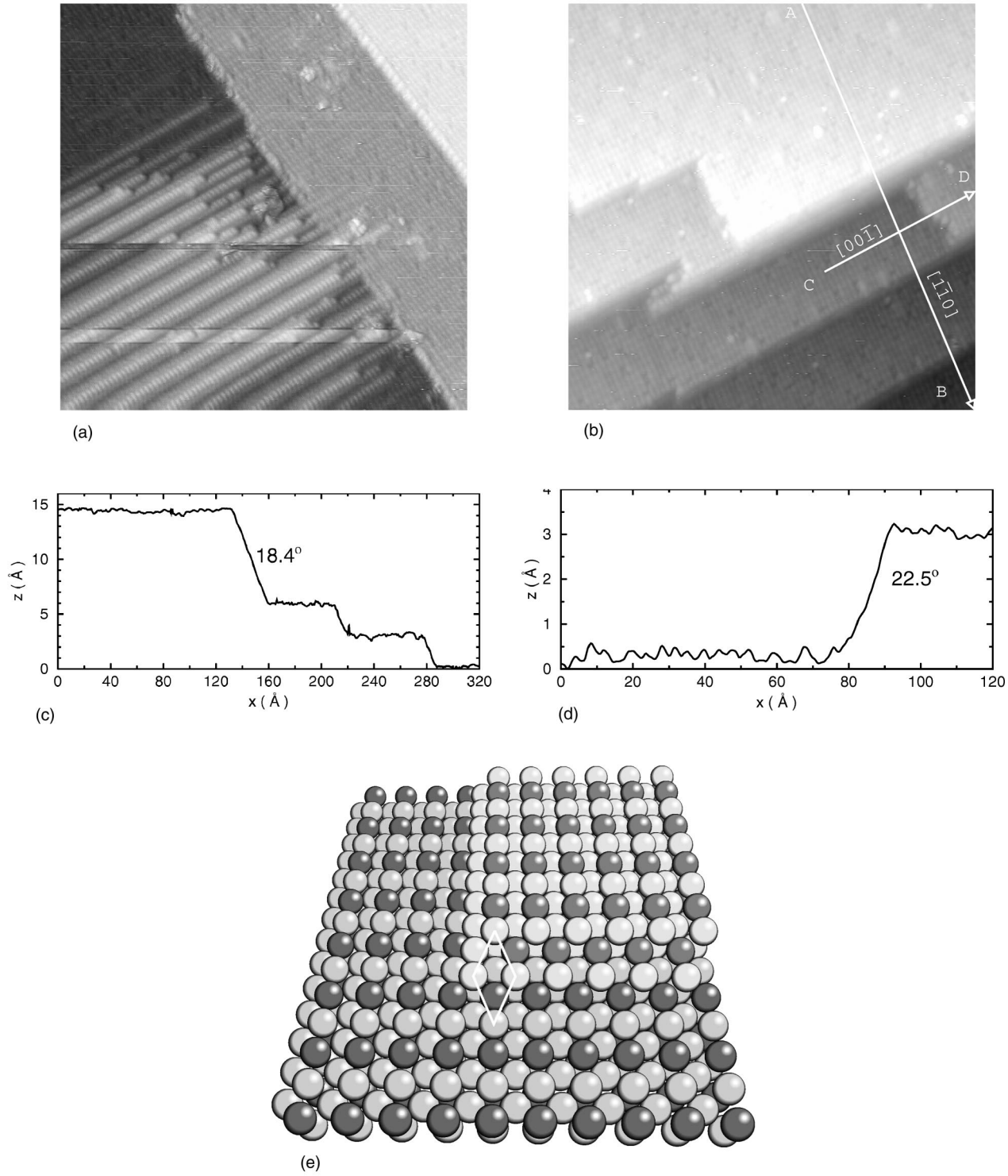


FIG. 6. STM images of coexisting faceted structures and flat terraces, $T_{\text{anneal}}=920$ K, 300 Å, 0.4 V, 0.8 nA (a), flat surface $T_{\text{anneal}}=920$ K, 300 Å, 0.5 V, 0.8 nA (b), with height scan between *A* and *B* along $[\bar{1}10]$ (c), and height scan between *C* and *D* along $[00\bar{1}]$ (d). Sphere model of double steps (e). Note that the minifacets along the $[\bar{1}10]$ double steps are {111} oriented and the multiple minifacets along the $[00\bar{1}]$ steps are {102} oriented as found on the real surface. At the {102} facets the structure model deviates from bulk termination, in accordance with the data.

$[00\bar{1}]$ rows in the {102} facets is 4.2 Å, i.e., *all* atoms in the measured outermost {102} layer are equally visible and have identical appearance. These observations apply to both the facets of the nonequilibrium surface after annealing to 715 K [Fig. 5(a)] and the facets of the $[00\bar{1}]$ steps on the equilibrium surface after annealing to 920 K [Fig. 7(b)]. We therefore conclude that the structure at the facets deviates from the bulk truncation. The outermost atomic layer of the facets,

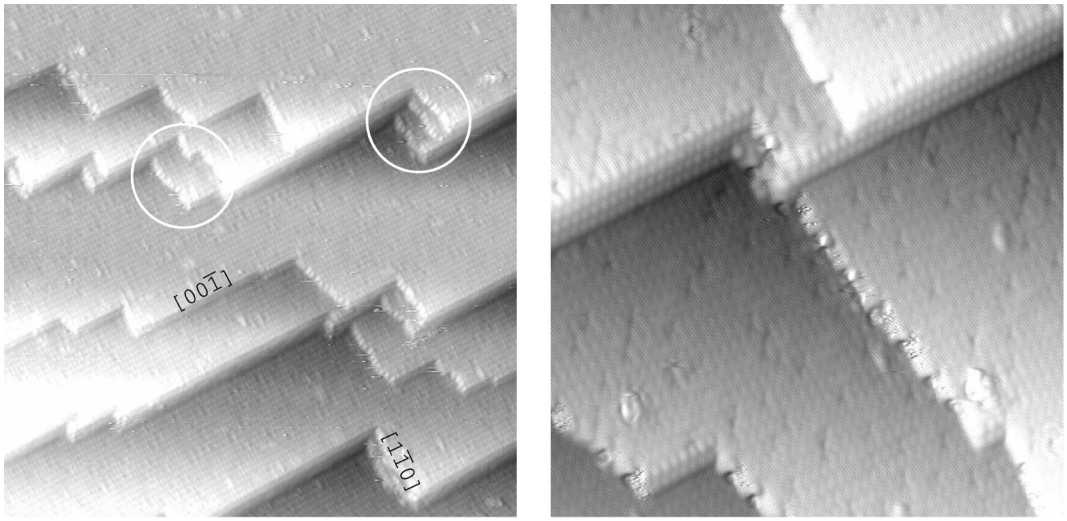


FIG. 7. STM images of merging double steps, 500 Å, 0.45 V, 0.8 nA (a) and 200 Å, 0.40 V, 0.8 nA (b). The $[00\bar{1}]$ steps form double, fourfold, and sixfold steps whereas the $[\bar{1}10]$ steps are predominantly double.

visible in the STM topography, contains only one elemental species. The atomic corrugation of these atoms indicates that this is Pt. The models in Figs. 5(c) and 6(e) are possible non-bulk-terminated structures for the facets of the hill-and-valley structure and at the $[00\bar{1}]$ step facets, which are in accordance with our data. The second layer in the model is pure Sn, in order to explain the high Sn concentration observed in the LEIS measurements.

Figure 8 shows an additional topographic feature of the well-annealed surface, i.e., single and a few double holes at Sn sites with an apparent depth of 1.0 Å relative to the height of ''normal'' Sn positions and 1.5 Å relative to the height of Pt positions. At the voltage of $+0.5$ V chosen in the STM image of Fig. 8 Pt is measured 0.5 Å higher than Sn. The corrugation amplitude at the bottom of the double holes is similar to the corrugation amplitude of Sn (0.3 Å, not visible in Fig. 8). At room temperature the mobility of the apparent holes is moderate. Whether these features are really Sn vacancies or rather Sn atoms at Pt sites in deeper layers is difficult to decide on the basis of STM imaging. In view of their extended apparent depth of 0.9 of the (110) interlayer distance the defects are probably real holes. Such holes should be quickly filled by atoms from the adatom gas. In this case, however, it is possible that the adatom gas is depleted in Sn due to the high vapor pressure of Sn, and the holes remain.

The difference in brightness of Sn and Pt is stronger at negative bias (filled states) than at positive (empty states). The change in contrast is shown in the STM image in Fig. 9 where the polarity of the bias (applied to the sample) is re-

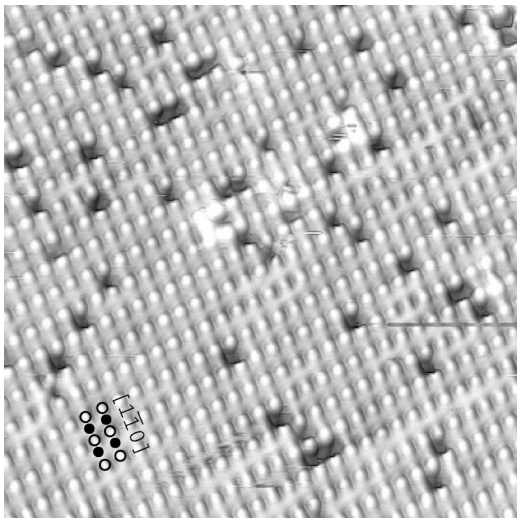


FIG. 8. STM image, 120 Å, 0.5 V, 0.8 nA. Pt atoms are visible as protrusions (open circles); Sn atoms are invisible (filled circles).

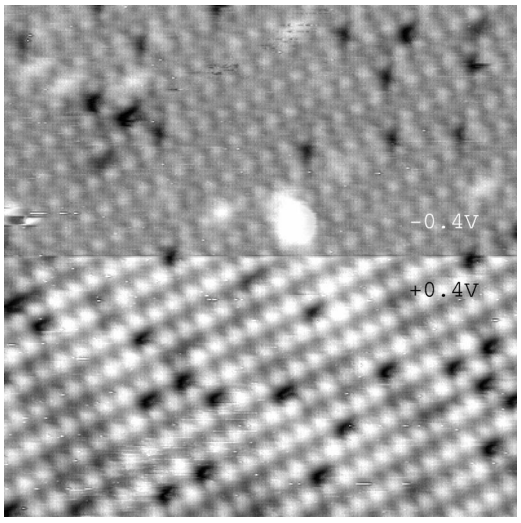


FIG. 9. STM image, 100 Å, $+0.4$ V (lower part), $-0.4$ V (upper part), 0.8 nA. The Pt atoms appear bigger when measuring the empty states (lower part). The contrast is higher when the filled states are measured (upper part). The big bump in the middle is presumably contamination.

TABLE I. Summary of the structures observed on $Pt_3Sn$ surfaces after annealing at moderate and high temperatures.

| Surface | 600–800 K | 1000–1100 K |
|---|---|---|
| (111) | $(\sqrt{3}\times\sqrt{3})R30°(Pt_2Sn)$, mesoscopic subsurface dislocation network | $p(2\times2)$, adatom islands |
| (100) | multiple row structure, pyramids bordered by {102} and {104} facets | $c(2\times2)$, double steps, single atomic adrows |
| (110) | hill-and-valley-like structure with {102} facets | $(2\times1)$, double steps, holes at Sn positions |

versed in the middle of the scan. This is in accordance with the calculated density of states.[5] Calculating the occupation of electronic states within small energy intervals below and above $E_F$ at the positions of the Sn and Pt atoms in the $Pt_3Sn$ structure gives higher charges for the Pt position. This estimation is done on the basis of band structure calculations, as in Ref. 5. The charge in the interval $[-0.4\ \text{eV},0\ \text{eV}]$ is 0.019 at the Sn atom and 0.25 at the Pt atom whereas the charge in the interval $[0\ \text{eV},+0.4\ \text{eV}]$ is 0.020 (Sn) and 0.071 (Pt). Thus, although the charge is always higher at the Pt atom, the ratio between the charges of Pt and Sn is enhanced for the filled states and higher contrast in STM images can be expected at negative bias.

## DISCUSSION

The structure of the $Pt_3Sn(110)$ surface is in line with that of the (111) (Ref. 4) and (001) (Ref. 5) surfaces as all three show the bulk structure termination after proper cleaning and annealing (Table I). Interestingly, all three surfaces respond to the depletion in Sn in the near surface region due to the sputter cleaning procedure by developing fascinating surface structures (Table I). The (111) surface shows a ''honeycomb'' network similar to that observed in heteroepitaxial films[15–18] and in the $Pt_xNi_{1-x}$ disordered alloy system.[19,20] The honeycomb structure is only observed when the (111) surface is $(\sqrt{3}\times\sqrt{3})R30°$ reconstructed, which implies a higher Sn concentration exclusively in the outermost layer compared to the fully annealed bulk-terminated $p(2\times2)$ structure. The (001) surface handles the Sn depletion in a very different way. At moderate annealing temperatures (600 K) the surface develops pyramidal structures with {102} and {104} facets. These structures disappear at higher temperatures (1000 K). The surface is then bulk terminated with double steps running parallel to the [100] and [010] surface directions. Single atomic Pt rows are found to remain on the surface oriented along the same directions. Here, on the (110) surface we find a faceting in the 600 K annealing regime. The facets have the {102} orientation like the faces of the pyramids on $Pt_3Sn(001)$. These {102} faces have no specific significance in the fcc crystal system. They occur when the step edges in each layer are situated one row behind the first possible bulk position (Fig. 6). They are composed of alternating {100} and (110) minifacets. Like the (110) plane they can exhibit PtSn or pure Pt termination. As the combination of LEIS and AES shows, the amount of Sn in the outermost layers of the faceted surface even exceeds that in the PtSn-terminated plain surface, whereas the deeper surface regions are depleted in Sn. The absolute values for the LEIS Pt/Sn ratio depend on the scattering azimuth. This can be explained by the large diameter of the shadow cone at low kinetic energies. Thereby most of the ions are focused on the channels, i.e., to the second layer, when impinging along the densely packed $[\bar{1}10]$ direction. This effect is less pronounced along $[00\bar{1}]$ and mainly the outermost layer is seen. With the faceted structure the polar angle perpendicular to the hills is only poorly definable. Shadowing of the Pt behind Sn might occur.

The hill-and-valley structure is very likely a result of stress compensation. Atomic relaxations can occur to a larger extent compared to a flat surface. This is important since the lattice constant of Pt rich regions is smaller than that of $Pt_3Sn$. Further, a gradual decrease in Sn depletion and stress with depth (except of the first layers) is assumed, which explains the relative low corrugation of the hill-and-valley structure of only a few angstroms. Obviously, the stress relaxation is anisotropic in the $Pt_3Sn(110)$ surface region, since it is rippled perpendicular to the $[00\bar{1}]$ direction. On the other hand the hill-and-valley structure can be assisted by remnant sputter damage.

It is surprising that the ripples on $Pt_3Sn(110)$ are along the densely packed $[\bar{1}10]$ direction and not perpendicular. In this way the exposed $[00\bar{1}]$ rows direction are elementally pure. This seems to be favored as on the plain surface the $[00\bar{1}]$ terrace edges in general run straight over large distances while the $[\bar{1}10]$ steps tend to curve (Fig. 7). This might be related to the strong binding between Pt and Sn. It is highly favorable that Pt is neighbored by Sn and vice versa, which implies that diffusion can be hindered along mixed chains such as $[1\bar{1}0]$. On pure fcc(110) surfaces, for instance Ag(110),[21] sputter induced hill-and-valley structures are parallel to the densely packed direction. These anisotropic structures are attributed to a balance between erosion rate during sputtering and anisotropic surface diffusion. This suggests that in the case of $Pt_3Sn(110)$ the surface diffusion is faster along the $[00\bar{1}]$ direction. In contrast to Ag(110),[21] the $Pt_3Sn(110)$ surface after sputtering is rough, independent of sputter time, angle of incidence of the ion beam, etc.

As LEIS shows[7] the bulk-terminated PtSn layer is exposed on the flat terraces of the well-annealed $Pt_3Sn(110)$

surface as on $Pt_3Sn(001)$. Note that with $Pt_3Sn(111)$ planes there is only one possibility of bulk truncation. Neither $Pt_3Sn(001)$ nor $Pt_3Sn(110)$ exhibits any steps with heights that correspond to an odd number of layers. The termination with the mixed layer on the (001) and (110) surfaces is under the constraint of chemical order also, in accordance with the surface energies of Sn (0.62 $J/m^2$) and Pt (2.7 $J/m^2$).[22] Annealing at 1000 K produces the bulk-terminated (110)(2 $\times$1) surface with double and some multiple double steps parallel to the $[00\bar{1}]$ and $[\bar{1}10]$ surface directions. For all surfaces we observe in the topographic STM mode that the Pt atoms are brighter than the Sn atoms in agreement with band structure properties.[5,23] A similar effect has been observed with $Pt_3Co$ alloys. In field-ion microscopy images Co is invisible between the Pt atoms.[24]

## SUMMARY

The $Pt_3Sn(110)$ surface has been investigated using STM, LEED, AES, and LEIS. As on the (111) and (001) faces, sputtering causes a depletion of the surface region in Sn. After annealing at 600 K LEIS and AES reveal a Sn rich outermost layer above a Pt rich subsurface region. In this regime STM images reveal a hill-and-valley structure consisting mainly of {102} facets. The previous reported additional spots in the LEED pattern[12] thus can be explained as facet spots. After annealing at 1000 K a bulk-truncated (2 $\times$1) surface is found. Of the two possible terminations (pure Pt vs PtSn) only the mixed one is realized; this is facilitated by steps that are formed only of even numbers of layers (double steps, etc.). The $[00\bar{1}]$ steps consist of {102} facets; they tend to merge and form larger facets. As these facets were also found on (001),[5] they seem to be energetically favorable in the $Pt_3Sn$ system in general. With STM the Sn atom cannot be imaged between Pt atoms as a bump since the local density of states at the Fermi edge is much lower for Sn than for Pt. This effect was found on (111) and (001) before and is in line with band structure calculations.[4,5,23]

## ACKNOWLEDGMENTS

This work was supported by the Deutsche Forschungsgemeinschaft (DFG) and the European Science Foundation (ESF) within the ALEnet project.

*Author to whom correspondence should be addressed. Electronic address: sspeller@uos.de

[1] R. Bowman, L.H. Toneman, and A.A. Holscher, Surf. Sci. **35**, 8 (1973).
[2] R.A. van Santen and W.M.H. Sachtler, J. Catal. **33**, 202 (1974).
[3] U. Bardi, Rep. Prog. Phys. **57**, 939 (1994).
[4] J. Kuntze, S. Speller, W. Heiland, A. Atrei, I. Spolveri, and U. Bardi, Phys. Rev. B **58**, R16 005 (1998).
[5] M. Hoheisel, J. Kuntze, S. Speller, A. Postnikov, W. Heiland, I. Spolveri, and U. Bardi, Phys. Rev. B **60**, 2033 (1999).
[6] A.N. Haner, P.N. Ross, and U. Bardi, Catal. Lett. **8**, 1 (1991).
[7] U. Bardi, L. Pedocchi, G. Rovida, A.N. Haner, and P.N. Ross, in *Fundamental Aspects of Heterogeneous Catalysis Studied by Particle Beams*, edited by H. H. Brongersma and R. A. van Santen (Plenum Press, New York, 1991), p. 939.
[8] A.N. Haner, P.N. Ross, and U. Bardi, Surf. Sci. **249**, 15 (1991).
[9] W.C.A.N. Celsen, A.W. Denier van der Gon, M.A. Reijme, H.H. Brongersma, I. Spolveri, A. Atrei, and U. Bardi, Surf. Sci. **406**, 264 (1998).
[10] A. Atrei, U. Bardi, G. Rovida, M. Torrini, and E. Zanazzi, Phys. Rev. B **46**, 1649 (1992).
[11] A. Atrei, U. Bardi, M. Torrini, E. Zanazzi, G. Rovida, H. Kasamura, and M. Kudo, Condens. Matter Phys. **5**, L207 (1993).
[12] A.N. Haner, P.N. Ross, and U. Bardi, in *The Structure of Surfaces III*, edited by S.Y. Tong, M.A. Van Hove, K. Takayanagi, and X.D. Xie (Springer, Berlin, 1991).
[13] J.M. MacLaren, J.B. Pendry, P.J. Rous, D.K. Saldin, G.A. Somorjai, M.A. van Hove, and D.D. Vvedensky, *Surface Crystallographic Handbook* (Reidel, Dordrecht, 1987).
[14] J. Kuntze, S. Speller, W. Heiland, P. Deurinck, C. Creemers, A. Atrei, and U. Bardi, Phys. Rev. B **60**, 9010 (1999).
[15] R. Stalder, H. Sirringhaus, N. Onda, and H. von Känel, Appl. Phys. Lett. **59**, 1960 (1991).
[16] H. Bethge, D. Heuer, Ch. Jensen, K. Reshöft, and U. Köhler, Surf. Sci. **331-333**, 878 (1995).
[17] H.J.G. Belk, J.L. Sudijino, H. Yamaguchi, X.M. Zhang, D.W. Pashley, C.F. McConville, T.S. Jones, and B.A. Joyce, J. Vac. Sci. Technol. A **15**, 915 (1998).
[18] H. Brune, Surf. Sci. Rep. **31**, 121 (1998).
[19] M. Schmid, A. Biedermann, H. Stadler, C. Slama, and P. Varga, Appl. Phys. A: Solids Surf. **55**, 468 (1992).
[20] M. Schmid, A. Biedermann, C. Slama, H. Stadler, P. Weigand, and P. Varga, Nucl. Instrum. Methods Phys. Res. B **82**, 259 (1993).
[21] S. Rusponi, C. Boragno, and U. Valbusa, Phys. Rev. Lett. **78**, 2795 (1997).
[22] L. Vitos, A.V. Ruban, H.L. Skriver, and J. Kollár, Surf. Sci. **411**, 186 (1998).
[23] Š. Pick, Surf. Sci. **436**, 220 (1999).
[24] T.T. Tsong and E.W. Müller, J. Appl. Phys. **38**, 3531 (1967).